

LEWIS/GRANT/IN-33

55648  
32 P.

LEO High Voltage Solar Array Arcing Response Model  
Interim Report - February, 1987

NAG 3-576

Roger N. Metz  
Dept. of Physics and Astronomy  
Colby College  
Waterville, Maine 04901

(NASA-CR-180073) LEO HIGH VOLTAGE SOLAR  
ARRAY ARCING RESPONSE MODEL Interim Report,  
Feb. 1987 (Colby Coll.) 32 p CSCL 09A

N87-16971

Unclas

G3/33 43926

LED High Voltage Solar Array Arcing Response Model  
Interim Report - February, 1987

NAG 3-576

Roger N. Metz  
Dept. of Physics and Astronomy  
Colby College  
Waterville, Maine 04901

## I. Introduction

A series of mathematical models has been developed that describe the electrical behavior of a large solar cell array floating electrically in the LEO space plasma and struck by an arc at a point of negative bias (refs. 1-3). There are now three models in this series: ARCI, which is a fully analytical, linearized model; ARCI, which is an extension of ARCI that includes solar cell inductance as well as load reactance; Non-linear ARC, which is a numerical model able to treat effects such as non-linearized, i.e., logarithmic solar cell I/V characteristics, conductance switching as a solar cell crosses plasma ground on a voltage excursion and non-ohmic plasma leakage current collection.

The ARCI model was developed in 1983-84 when the P.I. was a Visiting Scientist at NASA-Lewis. A grant, NAG 3-576, was awarded in the fall of 1984 for work in the summer of 1985 to enhance the ARCI model and to begin treatment of the non-linearities of the arc/array modeling problem. This work produced the ARCI model and the Non-linear ARC model. In the fall of 1985, NAG3-576 was continued with the goal of improving the Non-linear ARC model during the summer of 1986. The report presented here covers improvements made during summer 1986 and January, 1987.

## II. Work Proposed and Accomplished in 1986 under NAG 3-576

1) Proposed: "Write the model programs in a compiled computer language such as FORTRAN 77, PASCAL, or C so as to speed up execution."

Accomplished: The programs comprising the Non-linear ARC model were first converted from MBASIC to CBASIC. Execution was maintained on the Kaypro computer. Although this reprogramming was done in order to take advantage of the increased speed thought to be available in CBASIC, which is a compiled rather than an interpreted language, processing time actually increased. CBASIC carries 14 decimal digits for floating point numbers while MBASIC carries only 8. Apparently the extra digits carried by CBASIC more than offset any speed gains made by the compilation process in CBASIC. As a next step, the programs were converted to FORTRAN 77 for execution on Colby's VAX 8200 computer. This was entirely satisfactory and run times were ultimately reduced from one day (Kaypro) to several minutes (VAX).

2) Proposed: "Improve the convergence algorithms to permit solutions of increasing non-linearity. This would include, particularly, solutions with many back-biased cells."

Accomplished: Convergence was improved in several ways:

a) A hybrid of Newton's method and divide-by-2 search algorithms

was adopted both for  $V^-$  and for  $I^-$ , the two parameters that must be determined in order to achieve a solution to the circuit equations of the model at any point in time.

b) Look-ahead algorithms based on least-squares projections over the last four time steps were developed for  $V^-$ ,  $V^+$  and  $I^-$ .

c) Major portions of the calculations were coded in double-precision variables.

d) A hierarchy of imbedded print diagnostics was programmed so that divergent runs could be analysed when they occurred without burdening convergent runs with unnecessary I/O. This speeded execution.

The state of convergence of model runs is now sufficient to permit solutions routinely showing 10% back-bias of the array. A few runs have been made with more than 50% back-bias of the array at some time points. Also, the double precision analysis has largely removed the numerical oscillations of the transient solutions formerly found on the relaxation side of transient peaks in some runs.

3) Proposed: "Investigate non-ohmic plasma current collection, e.g., fractional power-law dependence on voltage as in non-spherical Langmuir Probe collection or 'flash-over' collection."

Accomplished: Model runs were made with plasma currents of the form:  $I = AJ_{th}(1+eV/kT)^p$ . This collection formula was applied to both the electrons and ions with  $T_e = 2T_i = .2$  e.v. and  $p = 0.5, 1, \text{ or } 1.2$ . Runs with a "flash-over" collection function were not done for lack of time although such functions should be treatable by the model.

4) Proposed: "Make sufficient runs of the numerical model to span the parameter spaces of interest and present the results of these runs in concise, graphical form."

Accomplished: More than 200 runs of the Non-linear ARC model have been made. Some of the results of the runs are presented in Figures 0 - 10 and Tables 1 - 4. Runs have been made for all 9 pairs of plasma collection exponents,  $p$ , described above; for plasma capacitances  $C_p = 1, 10$  and  $20$  pf; for fall-time constants,  $T = 10, 50, 100$  and  $1000$  microseconds; and for arc current amplitudes,  $I_a = 10-250$  amps.

A Hewlett-Packard Model 7475A computer driven plotter and software were purchased with grant funds and used to produce graphical output.

5) Proposed: "Use the experience gained with the expanded linear model to incorporate, insofar as possible, solar panel self-inductance and/or load reactance in the numerical model."

Accomplished: Solar panel self-inductance was included in the model in the form of an inductance placed in series with each solar cell. This inductance represents the cell's magnetic interactions with currents flowing in nearby chains of cells. Thus each solar cell is modeled as a non-linear resistance (i.e. logarithmic I/V characteristic) in series with an inductance and shunted by an inter-electrode capacitance. In addition, each cell has a capacitance to plasma ground in parallel with a conductance to plasma ground that is voltage-dependent. Runs in which the solar cell interelectrode capacitances and/or the cell series inductances are set to zero and model outputs compared to those using non-zero values to see if the parameters are important components of the model were not done for lack of time. These runs are planned for the near future.

The goal of including load reactance in Non-linear ARC was abandoned when it was realized how badly such a modification would affect the already difficult constraint equations, particularly the constraint that the instantaneous terminal voltage must equal the current through the load times the load impedance. The non-linearities of the various parts of the model conspire to make convergence unstable in even the resistive load impedance case for some runs that push the model to its limits. If further development is desired along this direction, new time resources will have to be applied to it.

In addition to the above proposals, which were made as part of the grant continuation application submitted in 1985, two other tasks were suggested by Drs. Snyder and Purvis when the P.I. visited NASA-Lewis prior to work in the summer of 1986. These were (a) to use the ARCIII extended analytical model to investigate the response to a given arc as the tuned frequency of the reactive load is varied and (b) to use the ARCII and/or ARCIII models to investigate response to a given arc as the operating point of array is varied from 80% to 100% of maximum power. Both of these studies were accomplished. The results will be described below. Bishwa Basnet, a student assistant who was hired using grant funds, made the necessary computer runs for these studies.

### III. Discussion of Results of Runs using the Non-linear ARC Model

All model runs reported here assume solar cells whose I/V characteristic curve is given by:  $V = A \ln(I-B) + C$  where  $A = 40\text{mv}$ ,  $B = 132.3\text{ ma}$  and  $C = 355\text{ mv}$ . This is the characteristic of a  $2\text{cm} \times 2\text{cm}$  silicon solar cell under full solar illumination. With the exception of runs reported in Tables 1 - 4, all runs assume plasma collection current powers,  $p = 1$ , for both electrons and ions. Thus, the spherical Langmuir Probe collection model has been assumed for both species for these runs. Runs with a 5 e.v. atomic oxygen ram collection for ions have been made as well as runs with fully thermal plasmas and  $p \neq 1$  for both ions and electrons. These are reported in Tables 1 - 4.

The  $t=0$  or quiescent solutions of the model equations describe a  $1000 \times 1500$  solar cell array that, in the absence of plasma interactions, makes 82KW of power at 450V at maximum (subsequently referred to as 100% power) or 66KW at 508V when operated at 80% of maximum on the high-voltage side (subsequently referred to as 80% power). The array consists of chains of cells that are wired in parallel. In this arrangement, the symmetry of the circuit permits one to focus on a single chain of cells that drives a load equal to the array load resistance times the number of chains,  $m$ . As indicated above  $m = 1500$  for the runs reported.

A load resistance is placed across the model array of the required magnitude to achieve quiescent operation at a chosen point in the absence of plasma. Plasma interactions change the operating points of the solar cells and cause the array to lose power to the plasma. The  $t=0$  or quiescent runs of the model calculate the power made in the presence of plasma, the power lost to the plasma and the power delivered to the load and checks that these are in agreement with each other. Tables 1 - 4 summarize the results of  $t=0$  runs made using different plasma collection assumptions. In all cases except those assuming ram collection, a thermal plasma with electron and ion densities of  $5 \times 10^{14}/\text{cc}$  and  $T_e = 2T_i = .2\text{ e.v.}$  is assumed. In ram cases, thermal electrons with  $T_e = .2\text{ e.v.}$  and ram ions with 5 e.v. of kinetic energy are assumed.

The quiescent array floats electrically in the plasma. Electrical equilibrium with the plasma is achieved using the requirement that the net plasma current collected by the array be zero. Different electron and ion collection models cause the array to float with different numbers of solar cells above plasma ground in voltage. A parameter, the "floating fraction", measures the number of cells above ground divided by the total number of cells in the array. The range floating fractions is 0 - 25% for runs reported here.

At  $t = 0$  the negative terminal of the array is assumed to be the site of an arc consisting of the ejection of electrons from the terminal. This point of arcing permits the symmetry of the quiescent solutions, in which all chains behave equally, to

carry-over to the time dependent solutions. The arc is imagined to have the form  $I(t) = I_0(\exp(t/T) - \exp(tK/T))$ , where  $T$  is the fall-time constant and  $K$  is a multiplier, always set to 5 in the runs reported here. Figure 0 shows the time dependences of two typical arcs,  $I(t)$ , used to drive the model. The arcs shown differ only in amplitude,  $I_0$ . In response to the arc, the model array undergoes a common-mode positive voltage swing associated with the charging of the array-to-plasma capacitances and also a differential mode, negative transient of the voltage across the load. The maximum of the load transient is denoted  $VT_{max}$  in the figures. Because all the  $VT_{max}$  are negative,  $|VT_{max}|$  values are plotted.

During the transient behavior of the array after the arc begins, the reactive elements of the circuit, which can be ignored in the quiescent solutions, come into play. All runs reported have used the value .02 microfarad for the interelectrode capacitance shunting each solar cell and the value 0.01 microhenry for the series inductance of each cell. The solar cell-to-plasma capacitances,  $C_p$ , are the same for all solar cells in the array and values of 1, 10 or 20 picofarads have been used.

Figure 1 shows the results of a single run of the model with an arc having  $I_0 = 100$  amps,  $T = 10$  microseconds,  $C_p = 10$  pf and  $p = 1$  for both electrons and ions. The quiescent operating point of the array is 80% power on the high voltage side.  $VT$  is the transient across the load,  $V+$  is the transient of the positive terminal of the array and  $V-$  is the transient of the negative terminal of the array. The arc used in this run is not sufficiently large that cells become back-biased at any time. One can see that the load transient,  $VT$ , has a maximum of only about 20V (negative) and that it rises and falls on a time scale comparable with that of the driving arc, which is given by the solid line in Figure 0. The transients for  $V+$  and  $V-$  are also small but they last considerably longer. In fact, they have not relaxed to zero out as far as  $t = 5T$ . Longer runs made with the model show that relaxation of all transients to zero ultimately takes place as it should.

Figure 2 shows the response of the same model array to a larger arc, given by the dotted line in Figure 0. Again the arc is not sufficient to cause back-biasing of cells. One can see that the transient response is greater for the larger arc, as one would expect. Figures 3 & 4 show the response to the same two arcs used in Figures 1 & 2 but with the quiescent operating point shifted to 100% power. For each arc, the transients at 100% power are larger than those for 80% power. This is primarily due to two effects. At 100% power the parallel combination of the internal dynamic resistance of the array with the load resistance is greater than the parallel combination of these resistances at 80% power. To a good approximation, at low arc current  $VT$  is given by the product of these parallel resistances and the arc current. Thus, the greater the parallel resistance the greater the values of  $VT$  for the same arc. In addition the arcs used in Figures 3 & 4 are large enough to cause back biasing of some cells (8% of

all cells in Figure 3 and 13% in Figure 4). Back-biasing is evidence that the cells have been pushed well into their non-linear operating regimes far from their quiescent operating points and near to their short-circuit-current points. Sharply increased load transients are the result of operation in this non-linear region because of the very high effective dynamic resistances of the cells there.

Without back-biasing the above parallel resistance model predicts that, for the same arc, the ratio of load transient maxima should go roughly as the ratio of parallel combinations of array internal and array load resistances calculated at the 80% and 100% operating points. This ratio of parallel resistances is 2.44 for runs shown in Figures 1-4. One can see that the ratio of  $V_{Tmax}$ 's for the 100 A arc as shown in Figures 1 & 3 is about 3.5 and that of the  $V_{Tmax}$ 's for the 150 A arc as shown in Figures 2 & 4 is about the same. Thus the transients in Figures 3 & 4 are larger than those to be expected from the parallel resistance model alone, i.e., from quiescent operating point dynamic resistance differences. The extra voltage swings are due to back-biasing of solar cells.

Figures 5 - 10 show maxima for load transients,  $V_{Tmax}$ , as a function of  $I_0$  for four different values of the fall-time constant,  $T$ , for three different values of the solar cell-to-plasma capacitance,  $C_p$  and for either 80% or 100% power. Figures 5 - 7 show 80% power results and Figures 8 - 10 show 100% power runs. In each figure, runs have been made with sufficiently large values of  $I_0$  to cause some, and sometimes many, solar cells to be back-biased at some point in time during the transient. The numbers in brackets beside the values of  $T$  in each figure show the maximum number of back-biased cells in a single chain (out of 1000) that occurred in runs with the greatest values of  $I_0$  shown. Runs at low values of  $I_0$  involve no back-biasing and runs at intermediate values involve some back-biasing but less than the maxima shown in brackets.

A linear model, such as ARC II, has the feature that the solutions for voltage transients due to arcs of the kind assumed here are proportional to the arc amplitude,  $I_0$ . Thus, plots of  $|V_{Tmax}|$  vs  $I_0$  for such models show straight-line dependence of  $|V_{Tmax}|$  on  $I_0$ . One can see in Figures 5 - 7 that  $V_{Tmax}$  is not a linear function of  $I_0$ . Indeed, if a straight line is fitted to the first few points, including zero, of the data for each curve, data points at higher values of  $I_0$  fall far above the line. This is further evidence that the non-linearities of the solar cells and/or the plasma interactions are at play for these runs.

Figures 5 - 7 refer to runs made at 80% power. One should notice that at this power, where the quiescent operating points of the solar cells are far from the non-linear region, sufficiently large arc currents can still cause quite dramatically large load transients. The maximum arc currents shown are sufficient to drive some cells from their 80% power



ORIGINAL PAGE IS  
OF POOR QUALITY

operating points into their non-linear regions and back-bias them.

The common-mode transients for the runs shown in Figures 5 - 7 are not given. They can be quite large. Their general behavior is the same as that shown in Figures 1 - 4, i.e., positive voltage excursions of both terminals with a relaxation to zero at times generally long compared to the arc fall-time constant,  $T$ . When  $T = 1$  ms, however, the other time constants of the array circuit are so much smaller than  $T$  that the transient responses to an arc are given approximately by ignoring all reactances. In this case all the transients follow the arc current in time. Figures 5 - 7 also show that for a given arc current amplitude  $VT_{max}$  depends on  $T$ . Usually  $VT_{max}$  increases with  $T$  for the same  $I_0$ , although not always. This dependence is not understood and needs more study.

Figures 8 - 10 show results for runs made with an array operating at 100% power. One sees in these figures that the values of  $I_0$  needed to produce back-biasing are smaller than they are at 80% power, as expected. The 100% power operating points have higher dynamic resistances and are closer to the non-linear region of the solar cell I/V characteristic than are the 80% power operating points. Thus a smaller arc current can cause a substantial load transient and can move the cells into the non-linear region. One also notices in these figures that the curves for given values of  $T$  and of  $C_p$  are more nearly linear than those in Figures 5 - 7. This is probably the result of limiting the values of  $I_0$  in most of these runs to those not producing high numbers of back biased cells, thus generating little non-linearity. However, there are some inconsistencies. In Figure 8, for example, the curve for  $T = 50$  microseconds is much more non-linear than that for  $T = 100$  microseconds yet the latter curve terminates in a run having 22% back-bias at some point while the former terminates in a run having only 15% back-bias.

Figures 8 & 9 show behavior in which  $VT_{max}/I_0 \sim 1$  ohm. This is within 20% of the parallel combination of array internal resistance at 100% power and the load resistance. Thus, for these runs, the load transients can be thought of roughly as arising from the arc current flowing through this parallel resistance, as suggested above. However, Figure 10 does not show this behavior except for the  $T = 1$  ms case. By comparison, at 80% power as shown in Figures 5 - 7, the parallel combination of resistances is about .5 ohm. One can see in these figures that, at least for low to intermediate values of  $I_0$ ,  $VT_{max}$  is also given very roughly by this parallel resistance times  $I_0$ . Thus, the rule-of-thumb that  $VT_{max} = I_0 \times (\text{array internal resistance in parallel with the load resistance})$  is a useful one in the absence of strong back-biasing.

Tables 1 - 4 show the results of 72 runs in which different plasma collection assumptions were made within the power-law model described above. Runs were made at each of three value of  $p$  for each species. These values of  $p$  may be interpreted roughly as

follows:  $p = .5$  models a cylindrical Langmuir probe,  $p = 1$  models a spherical Langmuir probe and  $p = 1.2$  is the largest value of  $p$  for which convergent solutions could be produced, even using double precision variables. In each of the runs listed, after the  $t=0$  solution was found, the transient behavior was calculated in response to an arc having  $I_0 = 50$  A,  $T = 10$  microseconds,  $C_p = 10$  pf,  $K = 5$  and the usual values of solar cell interelectrode capacitance and series inductance. Tables 1 and 2 list runs made at 80% power and Tables 3 and 4 refer to runs made at 100% power. Both thermal and ram ion cases are tabulated.

In the tables, "FF" stands for the "floating fraction". "Pmade" stands for the power actually made by the array in the presence of the plasma interactions assumed in the run. "Ploss" stands for the power lost to plasma leakage currents. "VTmax" has the usual definition as the maximum of the load transient in a run and "BBCmax" is the maximum number of back-biased cells seen in a run.

The tables permit several overall observations to be made. First, floating fractions as high as 50% can occur if one uses a high collection power,  $p$ , for ions and a low power for the electrons. On the other hand, if the electrons are favored, the floating fraction approaches zero. Second, significant amounts of power can be lost to plasma interactions. More than 10% can be lost in worst cases where high values of  $p$  are used for both ions and electrons. Third, and most striking, at a given quiescent power level, the load transient maxima that are produced by the same arc are almost totally independent of the plasma collection assumptions and the floating fractions. It is as though the plasma interactions serve only to establish the floating state of the array. The arc then drives the load transient according to internal impedances of the array and the load and without regard to the plasma interactions. Clearly, this behavior cannot also be true for the common-mode transients since they depend on  $C_p$ , the cell-to-plasma capacitance.

#### IV. Discussion of Results Using the ARC III Model

About the beginning of summer, 1986, a decision was announced that the A.C. power system of the proposed Space Station is to be operated at a frequency of 20 Khz. Thus, the work that the P.I. reported in January, 1986 covering the development and use of the ARC III analytical model to study the effects of negative arc transients on a model solar cell array driving a 400 hz reactive load no longer relevant for the Space Station. Accordingly, the P.I. was asked to make some new runs of ARC III using 20 Khz as the tuned frequency. This was done during the summer of 1986. The results of these runs are summarized in Figures 11 - 14.

The ARC III model is an extension of the ARC II analytical model in which the resistive load of ARC II is replaced with an inductor set in series with the parallel combination of a

resistor and a capacitor so as to model the input stage of a simple D.C. to A.C. inverter. An inductance in series with each solar cell is also included in ARC III. The value of the load resistor is chosen, as in ARC II, to establish D.C. operation of the solar cell array at the desired operating points of the cells. The values of the load inductor and capacitor are chosen so that the load has resonant oscillations at the nominal A.C. frequency of the inverter being modeled by the reactive load and also that the energy drawn by the load per cycle of oscillation is a chosen fraction of the maximum stored energy in the load. For the runs reported in 1986, the load frequency was set at 400 Hz and the energy draw per cycle at 2%. The runs of ARC III reported here use the same 2% power draw but inverter frequencies from 400 Hz up to 20 KHz have been used.

These ARC III runs assume the same plasma as described above for the Non-linear arc runs. Collection of electrons and ions to the solar cells from the plasma is assumed to be ohmic, i.e., the collected current at each cell is assumed to be proportional to the voltage of a solar cell interconnect. For interconnect voltages  $\gg kT$ , i.e. almost everywhere on the array except very near plasma ground, this collection is just that used in the Non-linear model with  $p = 1$  for both ions and electrons.

The analytical models ARC II and ARC III are not able to treat the plasma interactions of solar cells individually. Rather, the plasma currents (represented by electron or ion conductances) and charge storage (represented by capacitances) associated with the solar cells are collected together in parallel into two groups. Each group is arbitrarily assigned to either the negative or the positive terminal of the array. This treatment gives estimates of the upper and lower limits to the effect of plasma interactions on the array during a negative-bias arc transient. The "plasma-split" parameter (PS) directs where the plasma conductances and capacitances are placed. If all the elements are grouped at the negative terminal,  $PS=0$ . If all are grouped at the positive terminal,  $PS=1$ .  $PS=.5$  is a 50/50 split.

Figures 11 and 12 show the results of runs of ARC III with the load reactance tuned for 20KHz and the power draw at 2%. The amplitude of the arc driving the model,  $I_0$ , is 10 amps in each case. Values of the plasma-split parameter, PS, and of the capacitance-to-plasma of each solar cell,  $C_p$ , are as shown for each set of data. The quiescent operating points of the solar cells is set at either 80% power on the high voltage side, ( $PF=.8$ ) or 100% power, ( $PF=1$ ).  $T$  is the fall-time constant of the arc current. The arc current multiplier,  $K$ , is set at 5. The inductance in series with each cell is .01 microhenry and the interelectrode capacitance in parallel is .02 microfarad.  $V_{Tmax}$  is the maximum of the transient voltage across load resistor during an arc that strikes the negative terminal of the array.

One notices several features in Figures 11 and 12 immediately. First, runs at the four different combinations of values of PS and  $C_p$  used yield remarkably similar results. This

feature has also been seen in some runs of the Non-linear model. Apparently the load transient is rather insensitive to the plasma interactions. The second feature is that  $|VT_{max}|$  rises with  $T$ . For values of  $T$  less than 50 microseconds, which is the period of the 20 KHz tuned load, this rise makes sense. As the arc time-constant comes into the range of the period of the tuned circuit, resonance should occur. However, for  $T$  greater than 50 microseconds, the values of  $|VT_{max}|$  should begin to die off. This is not seen, probably because the equations of ARC III assume that once the arc is over, i.e., in a few times  $T$ , the state of the system relaxes to what it was before the arc struck. For a load tuned to 400 Hz, which has a period of 2500 microseconds, this is a good approximation for values of  $T$  out to 100 microseconds, at least. However, when the load is tuned to 20 KHz, the approximation is not valid for fall-time constants greater than a few microseconds. Thus one expects that results in these figures cannot be trusted much past  $t = 10$  microseconds. One can say only that  $|VT_{max}|$  is greater when the load period matches the arc time-constant than it is when the load period is longer than the arc time-constant. A third observation is that the load transients do not show the usual dependence on solar cell operating point. This is not as yet understood.

Figures 13 and 14 show results of ARC III runs using the same plasma and arc parameters as used in Figures 11 and 12. In both figures  $C_p = 1\text{pf}$ . Figure 13 is for 80% power and Figure 14 for 100% power. The figures show values of  $|VT_{max}|/T$  calculated for arcs of different fall-time constants,  $T$ , as a function of the tuned frequency of the load. In the figures, there is a general trend upward of  $|VT_{max}|/T$  with load frequency. The data for  $T = 1$  microsecond (.001 msec) are good all the way out to  $f = 20$  KHz, i.e., the approximation mentioned above is valid. The same is true for the data at  $T = 10$  microseconds (.01ms). The  $T = 100$  microsecond data are probably good out to no more than 10 KHz and the 1ms data out to no more than 1 KHz.

Figures 13 and 14 are valid over a sufficient frequency range to suggest that ARC III makes a strong prediction that arcs with  $T = 1 - 100$  microseconds will produce larger transients on reactive loads tuned to 20 KHz than tuned to 400 Hz. Runs of ARC III shown suggest that for arcs with fall-time constants in this range, transients across the load resistor may be one to two orders of magnitude larger at 20 KHz than they would be at 400 Hz. On the other hand, multiplication by the appropriate values of  $T$  for each data set reveals that the magnitudes of the maxima of most of the load transients shown are really quite small, and are probably negligible, even though they are greater at 20 KHz than at 400 Hz. Once again one notes also that the load transient maxima are not very sensitive to the solar cell operating points, i.e., the results for 80% and 100% runs on otherwise identical parameter values do not differ markedly.

#### REFERENCES

1. R. N. Metz, "Circuit Transients Due to Negative Bias Arcs on a High Voltage Solar Array in Low Earth Orbit", NASA TP2407, AIAA 23rd Aerospace Sciences Meeting, Reno, Nevada, January, 1985.
2. R. N. Metz, "Circuit Transients due to Arcs on a High-Voltage Solar Array", Journal of Spacecraft and Rockets, Vol. 23., No. 5, Sept.- Oct., 1986.
3. R.N. Metz, "Circuit Transients Due to Negative Bias Arcs-II", AIAA 24th Aerospace Sciences Meeting, Reno, Nevada, January, 1986.

Fig.0 - Arc Currents vs t

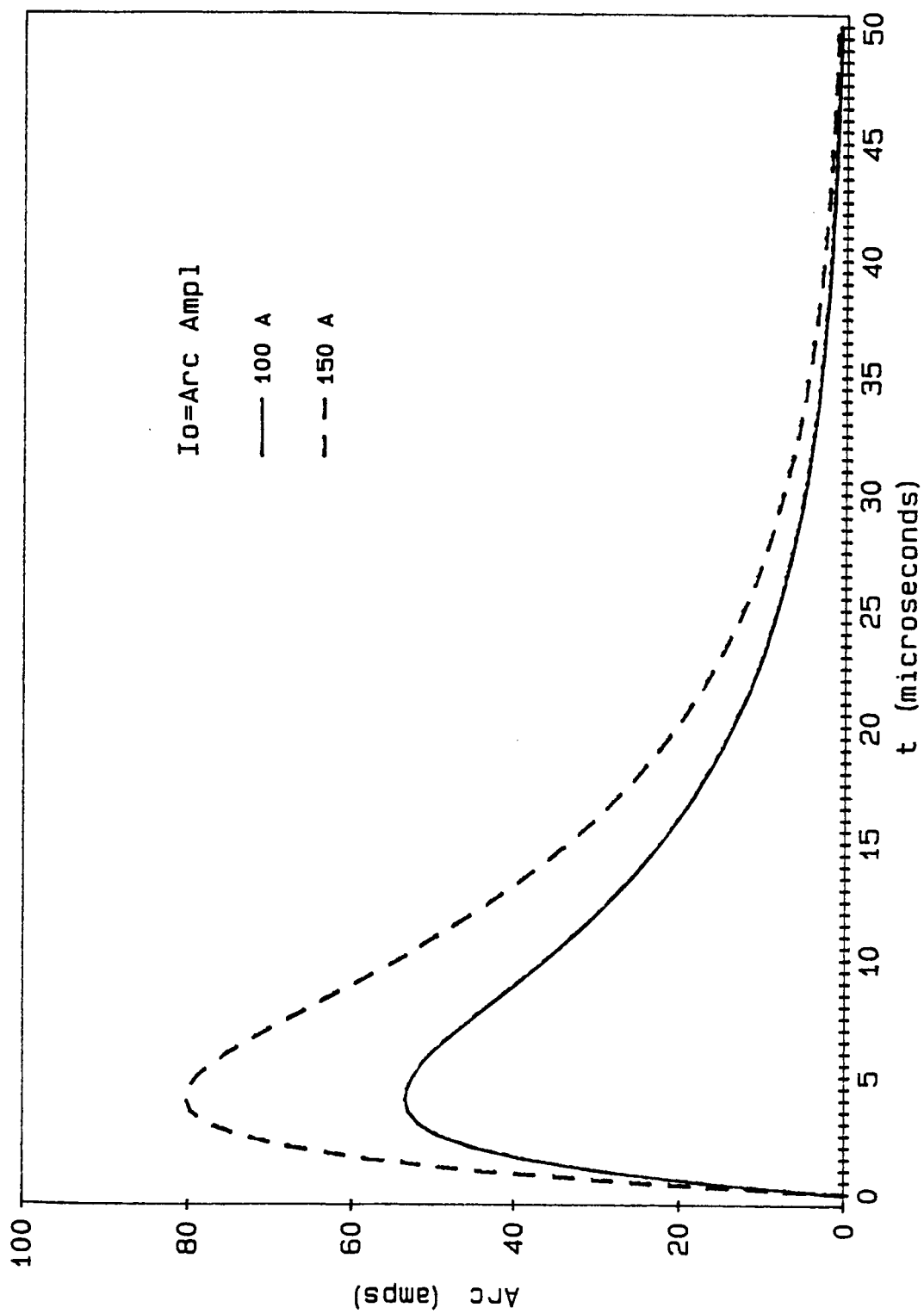


Fig.1 - Voltages vs t (pf=80%)

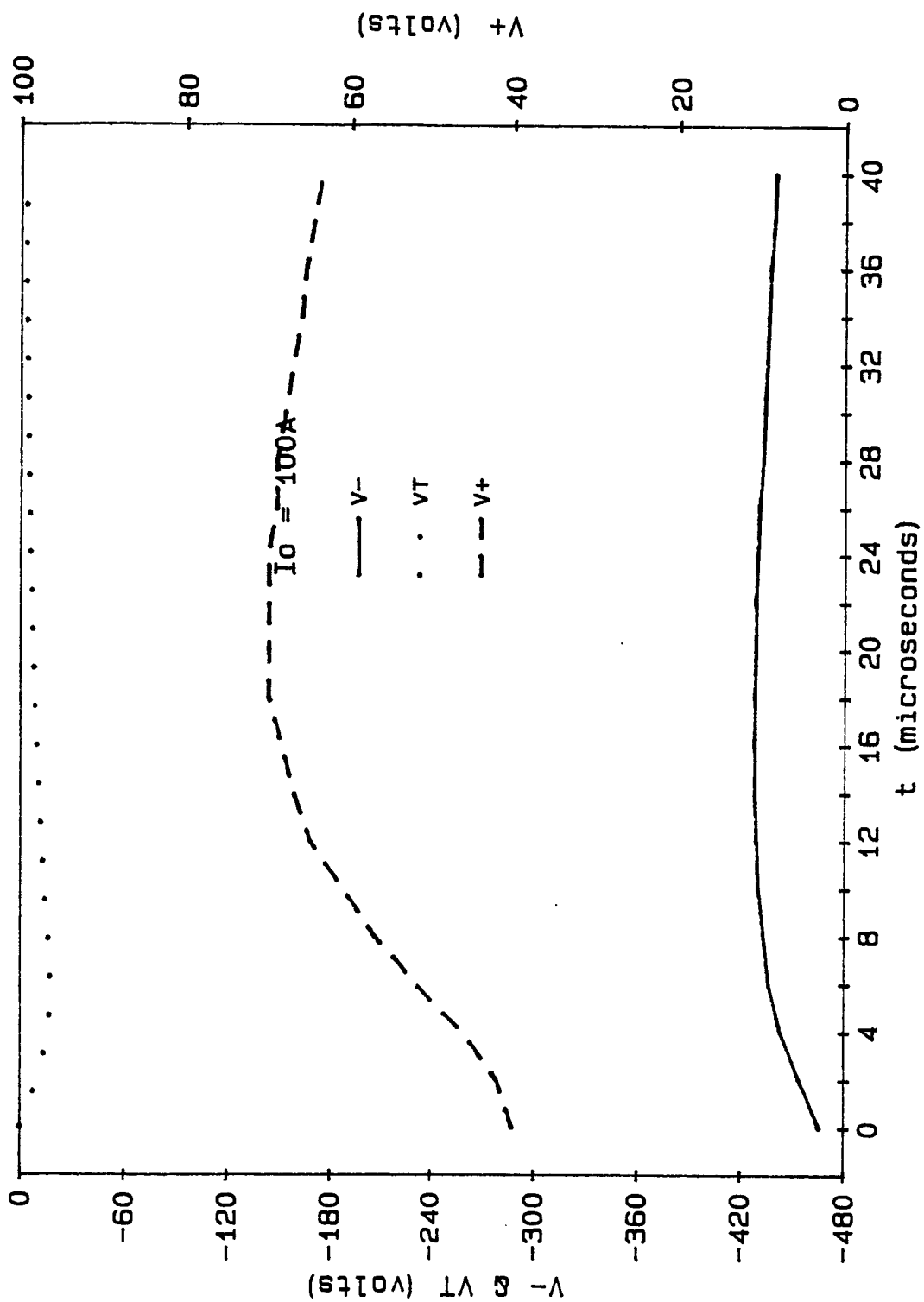


Fig.2 - Voltages vs t (pf=80%)

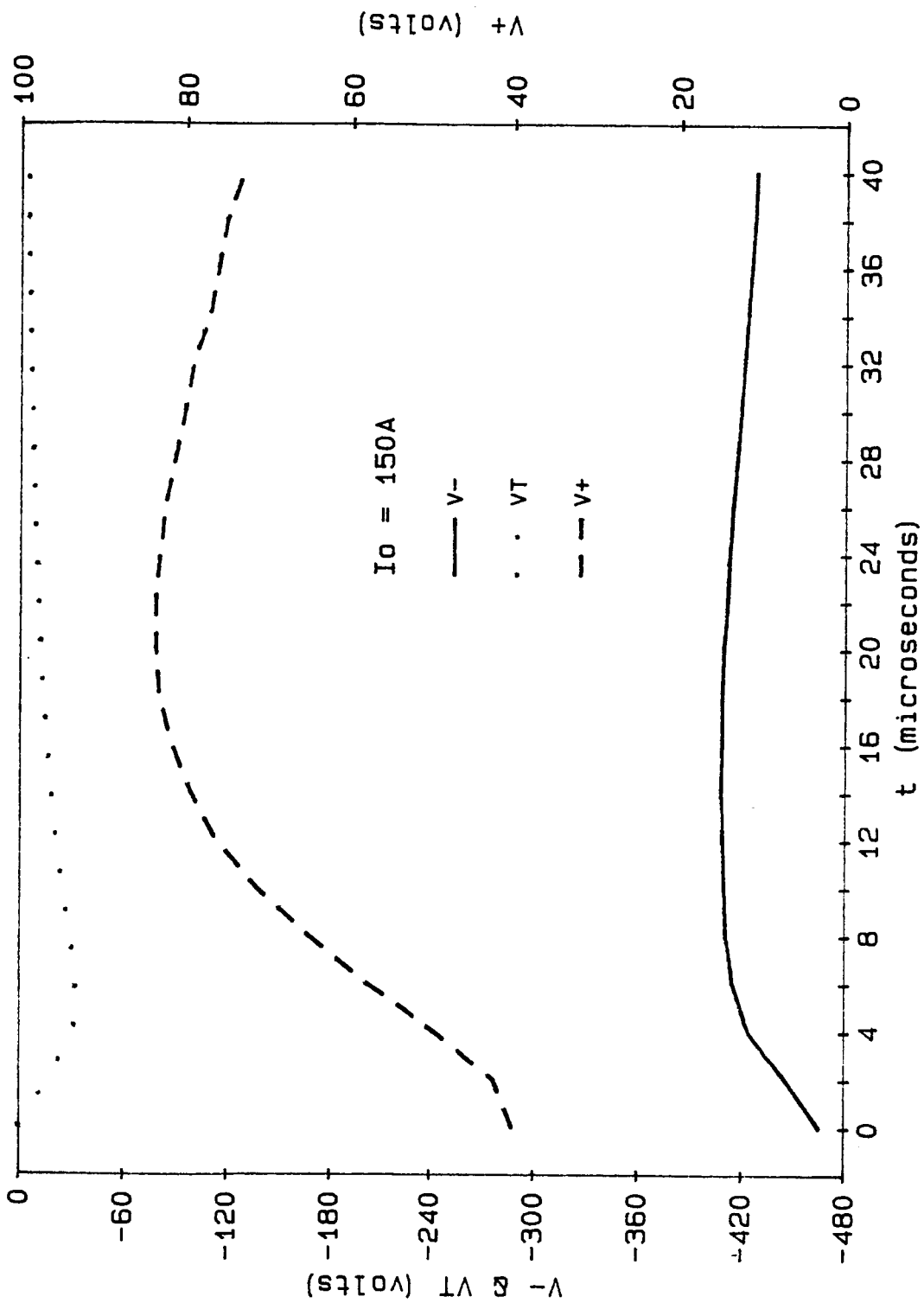




Fig.3 - Voltages vs t (pf=100%)

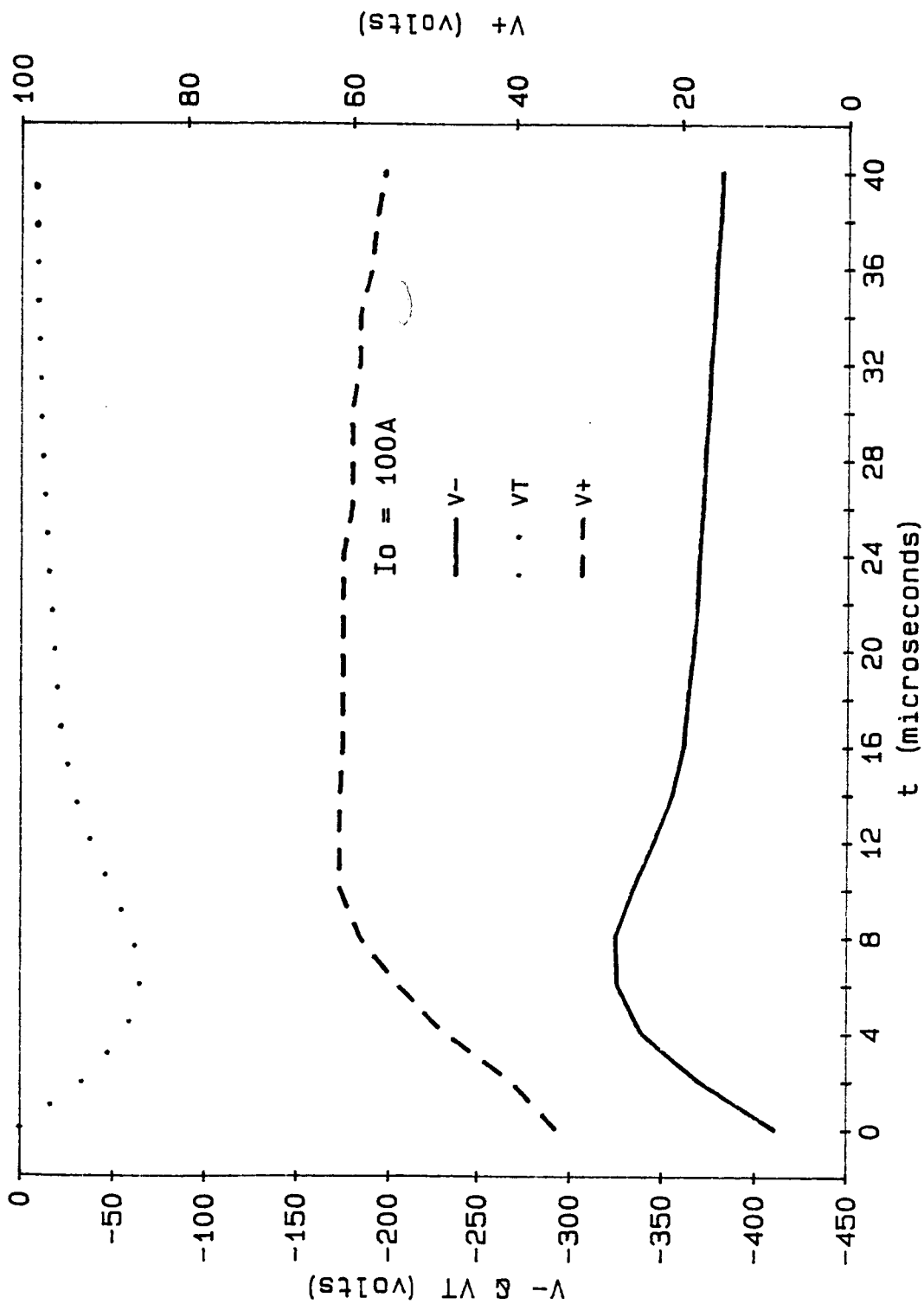


Fig.4 - Voltages vs t (pf=100%)

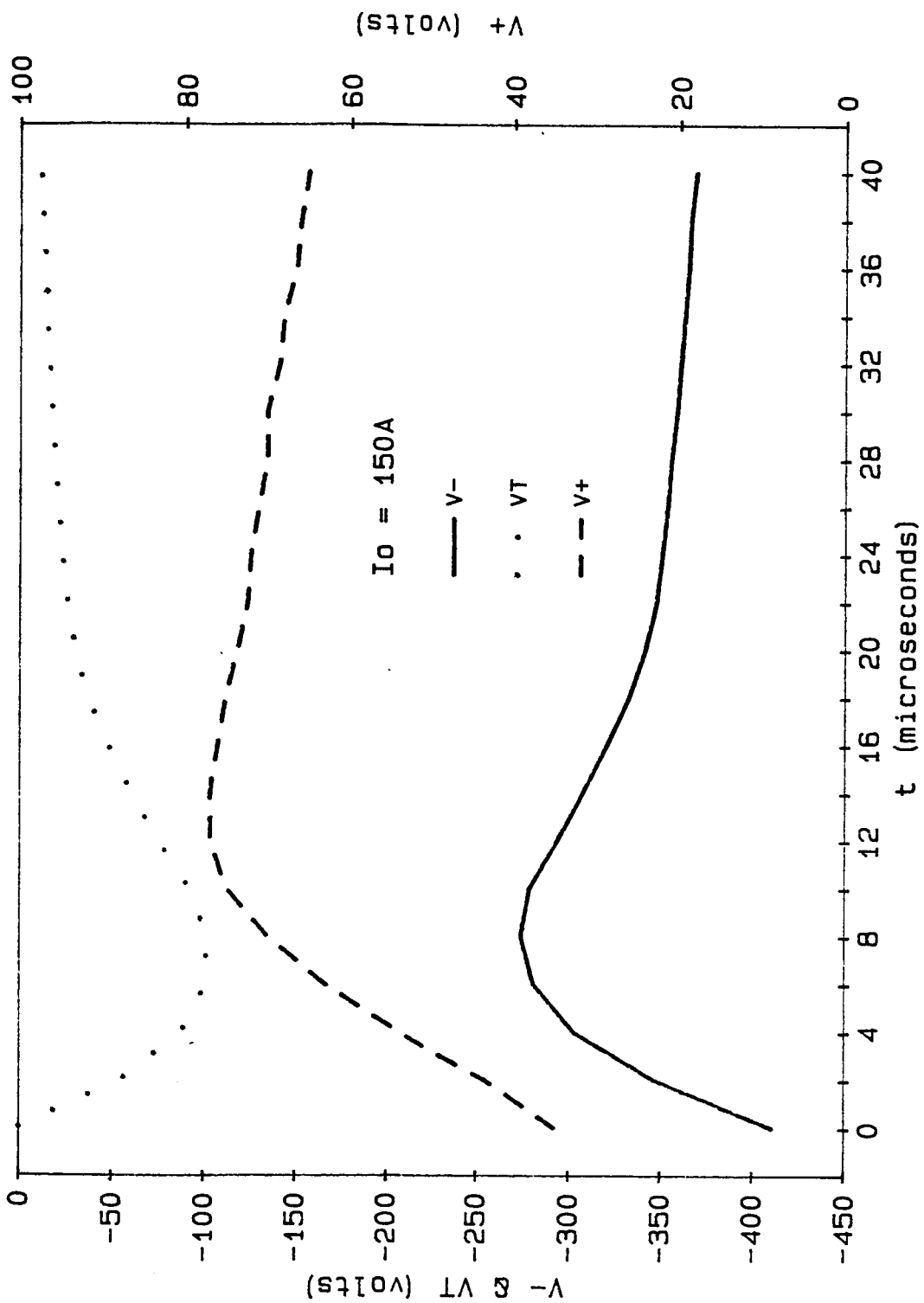


Fig.5 - VTmax vs Io (Cp=1pf)

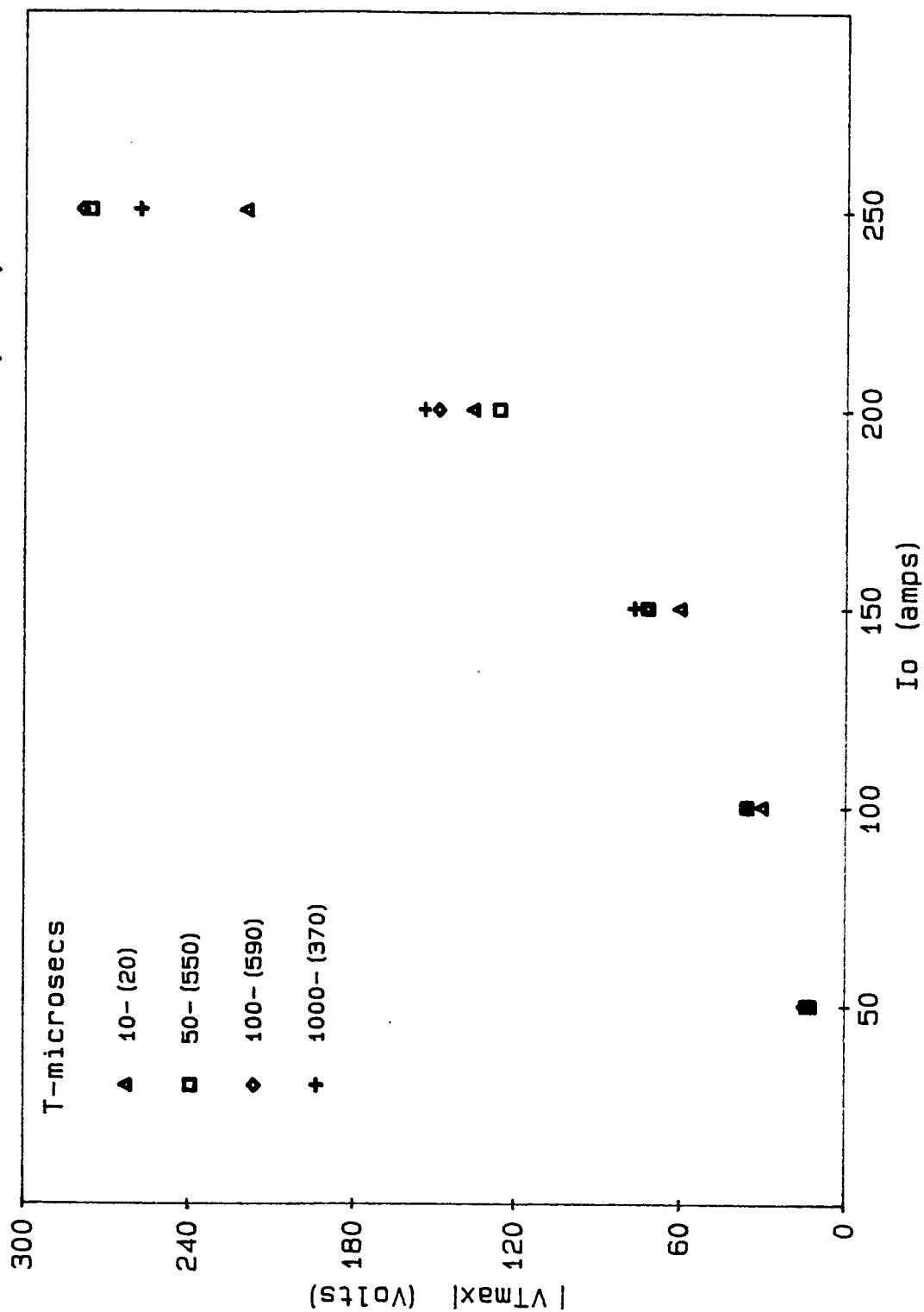


Fig.6 -  $V_{Tmax}$  vs  $I_o$  ( $C_p=10\text{pf}$ )

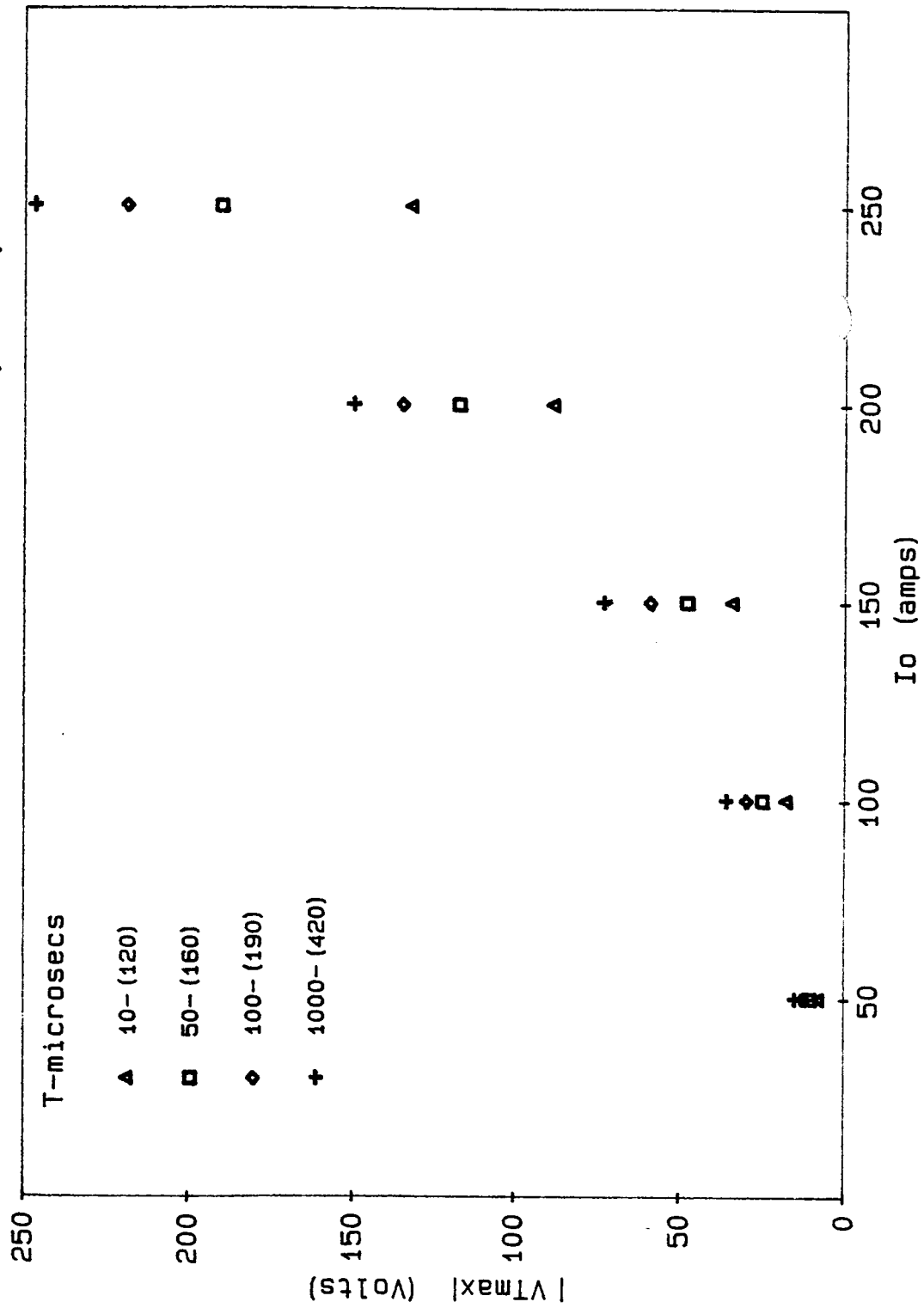


Fig. 7 -  $V_{Tmax}$  vs  $I_o$  ( $C_p=20pf$ )

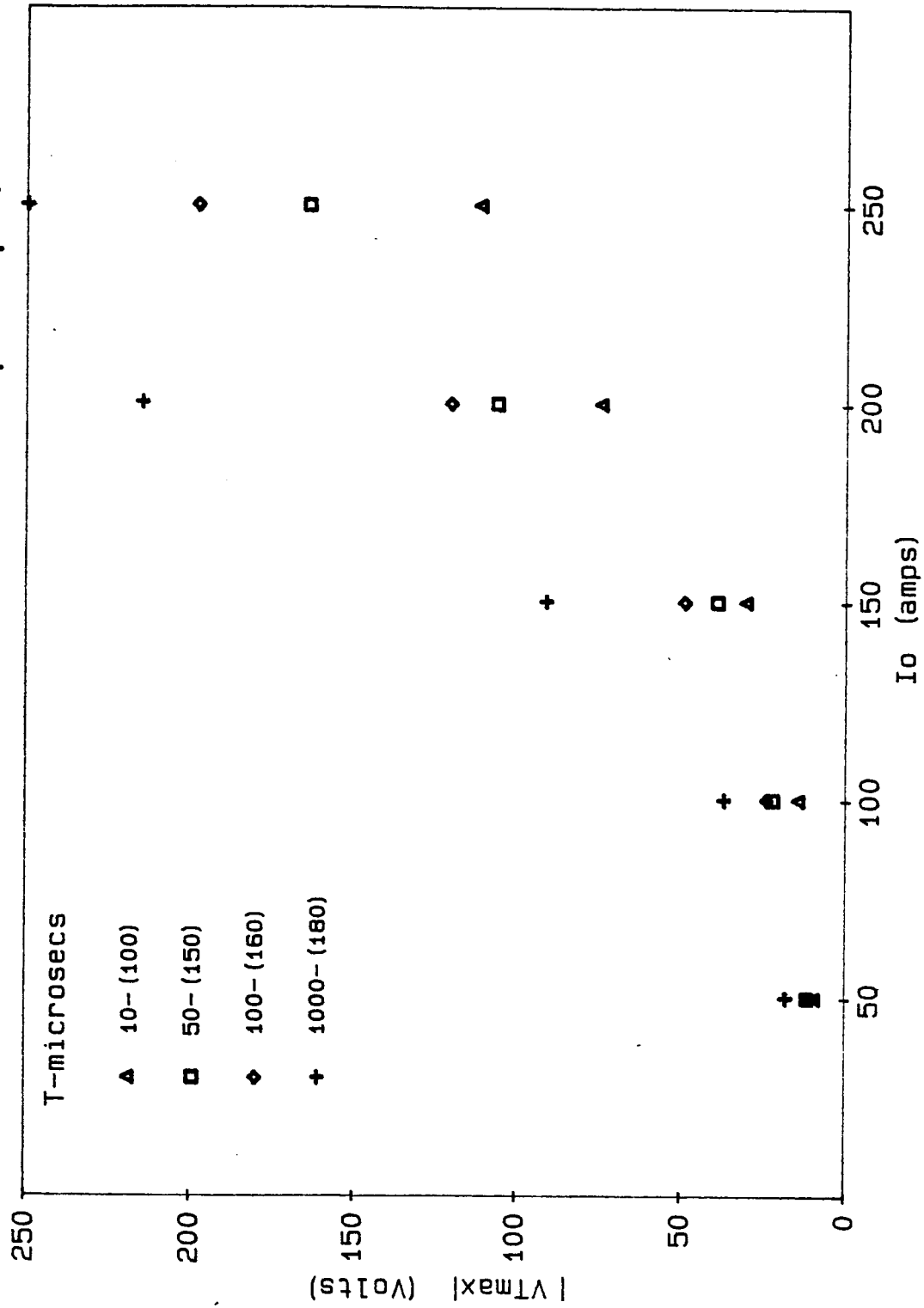


Fig.8 -  $V_{Tmax}$  vs  $I_0$  ( $C_p=1\text{pf}$ )

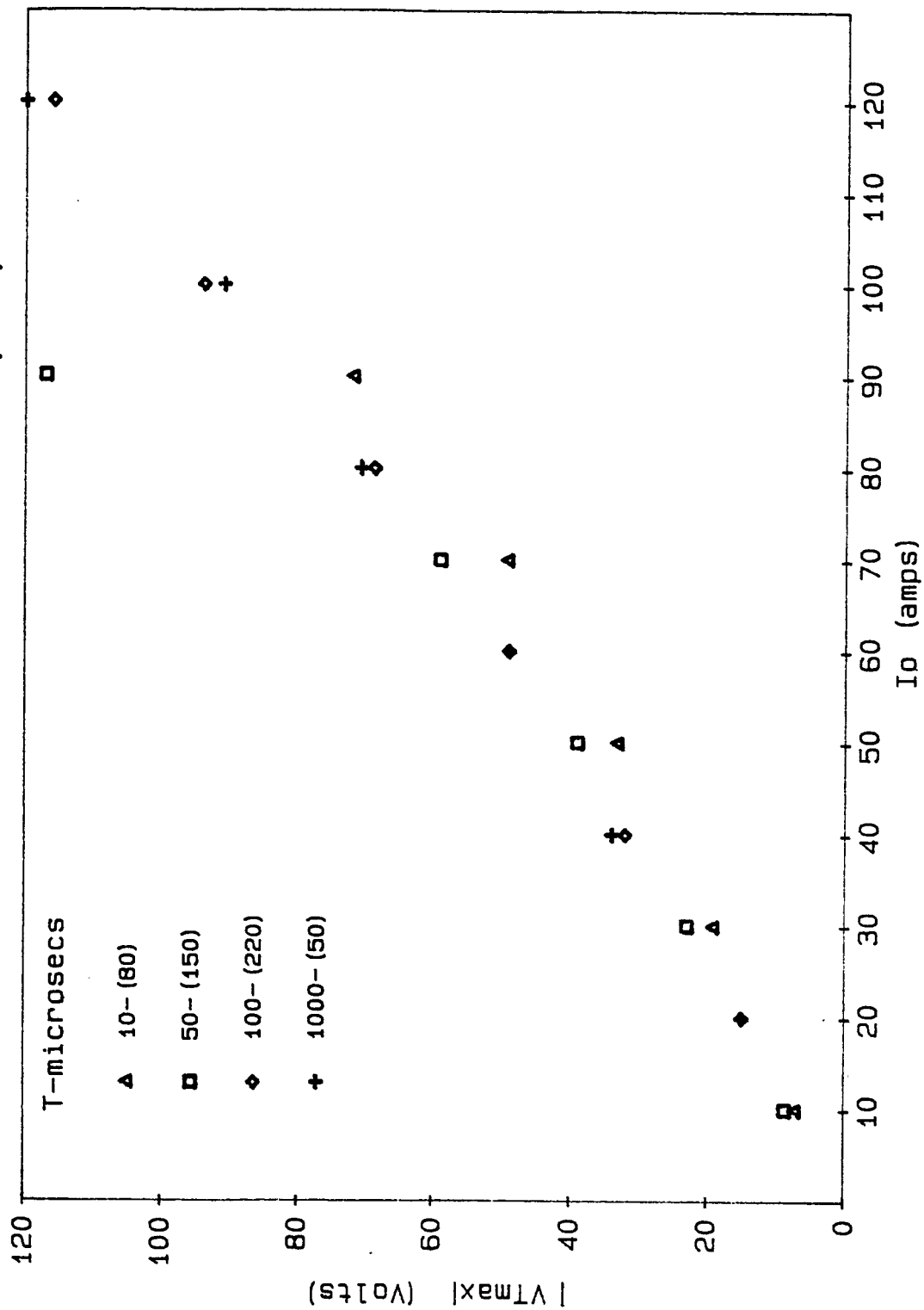


Fig. 9 -  $V_{Tmax}$  vs  $I_o$  ( $C_p=10\text{pf}$ )

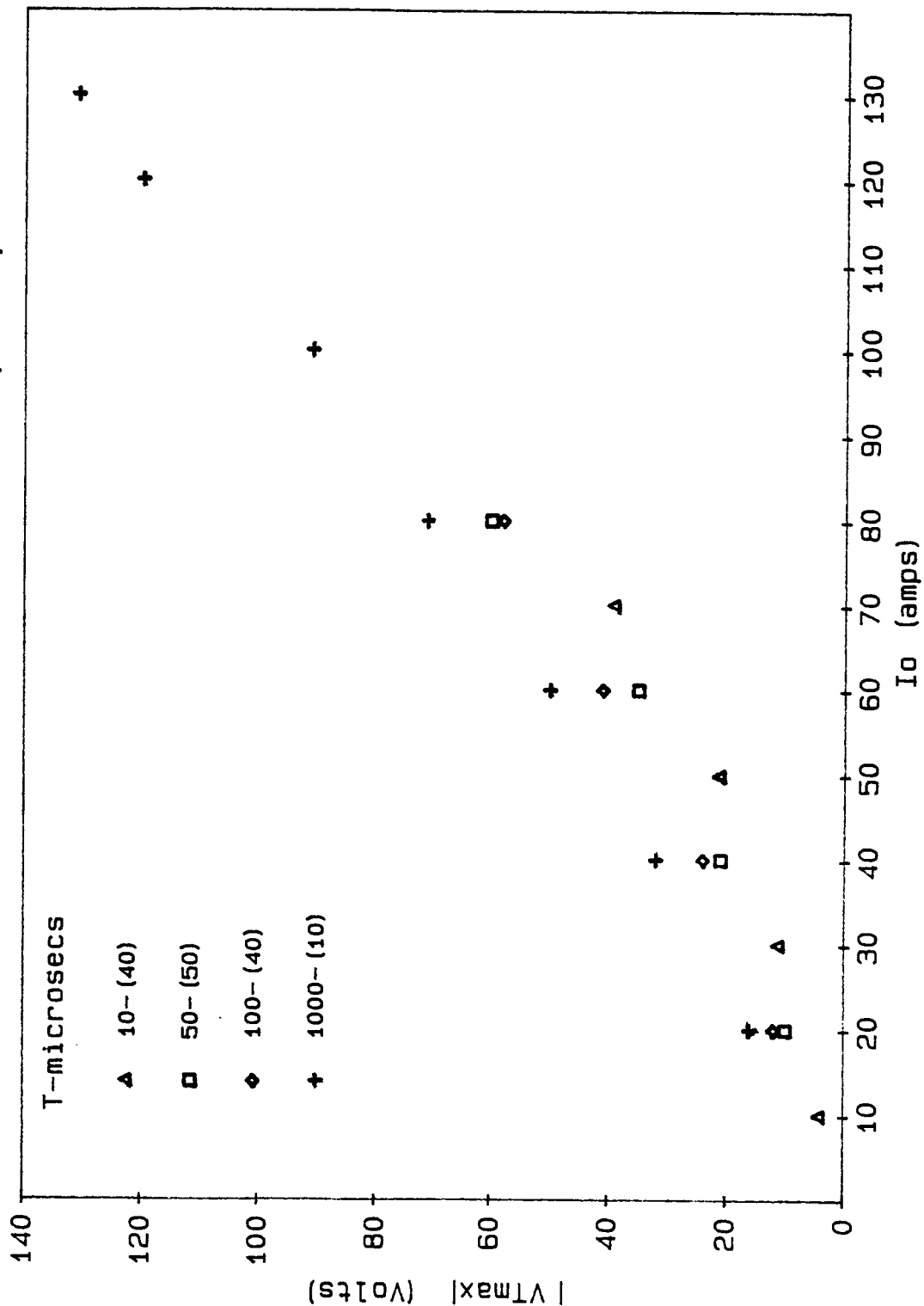


Fig.10 -  $V_{Tmax}$  vs  $I_o$  ( $C_p=20pf$ )

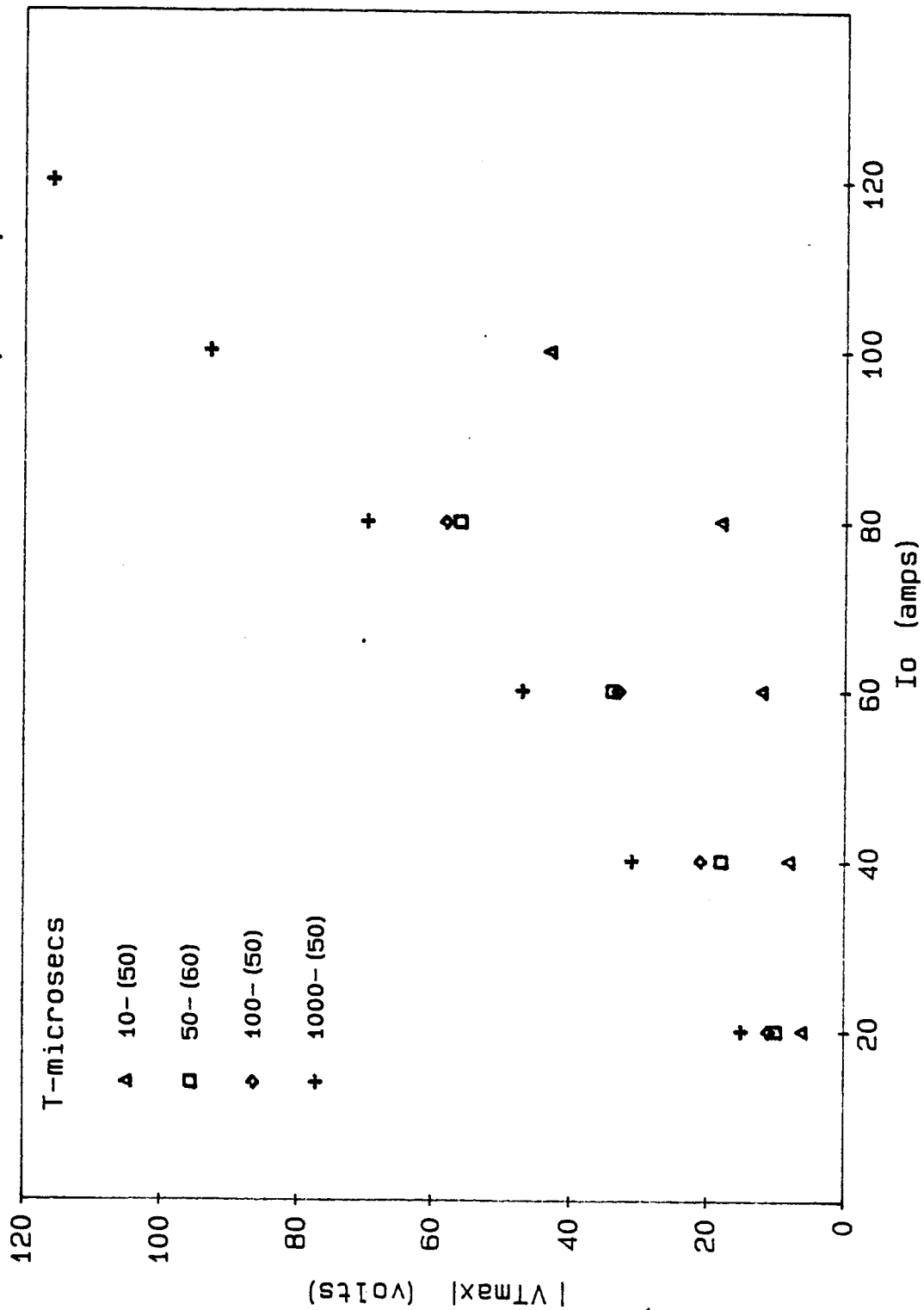




FIG.11 -  $V_{Tmax}$  vs T at 20 KHz (PF=.8)

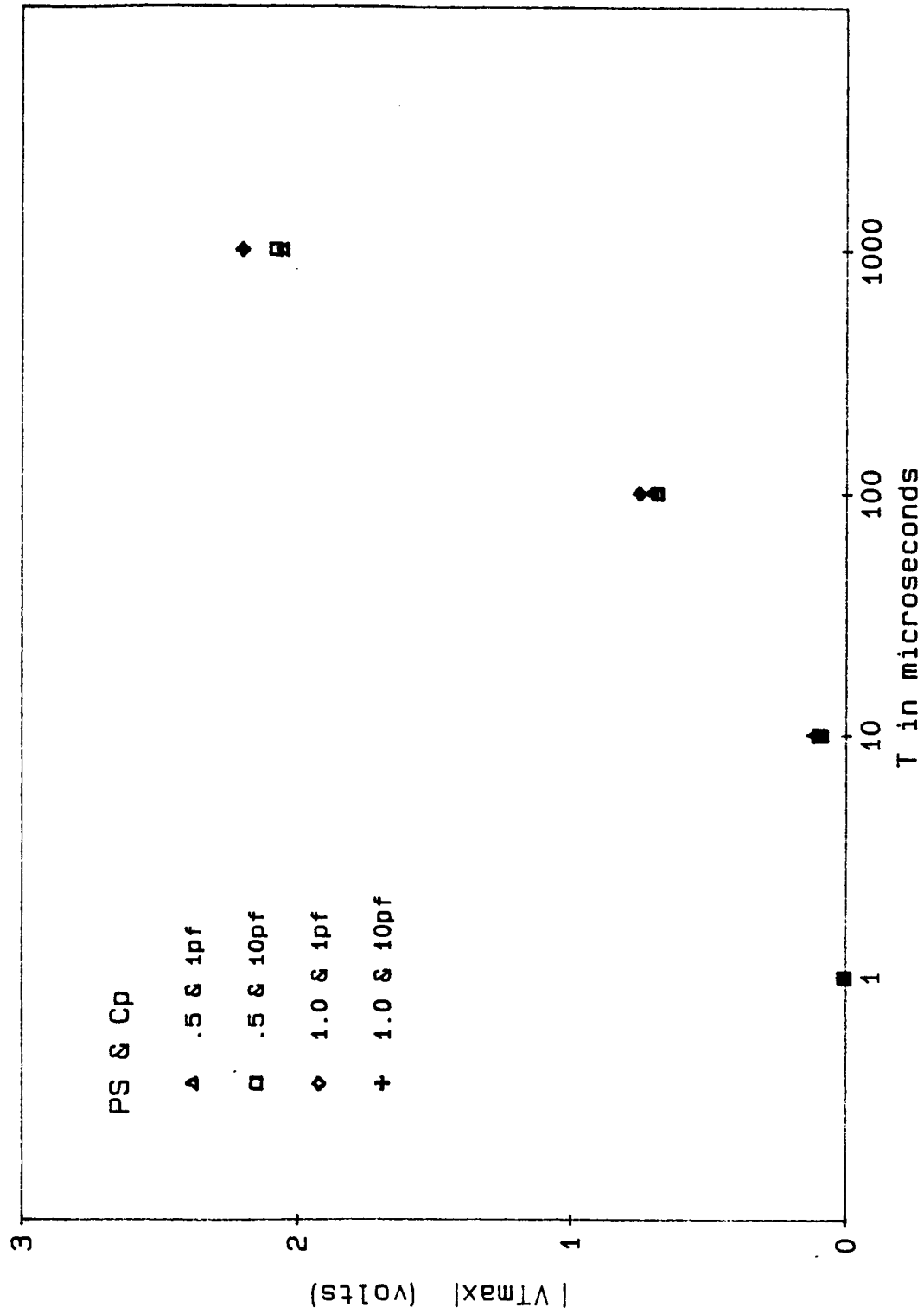


FIG.12 -  $V_{Tmax}$  vs T at 20 KHz (PF=1)

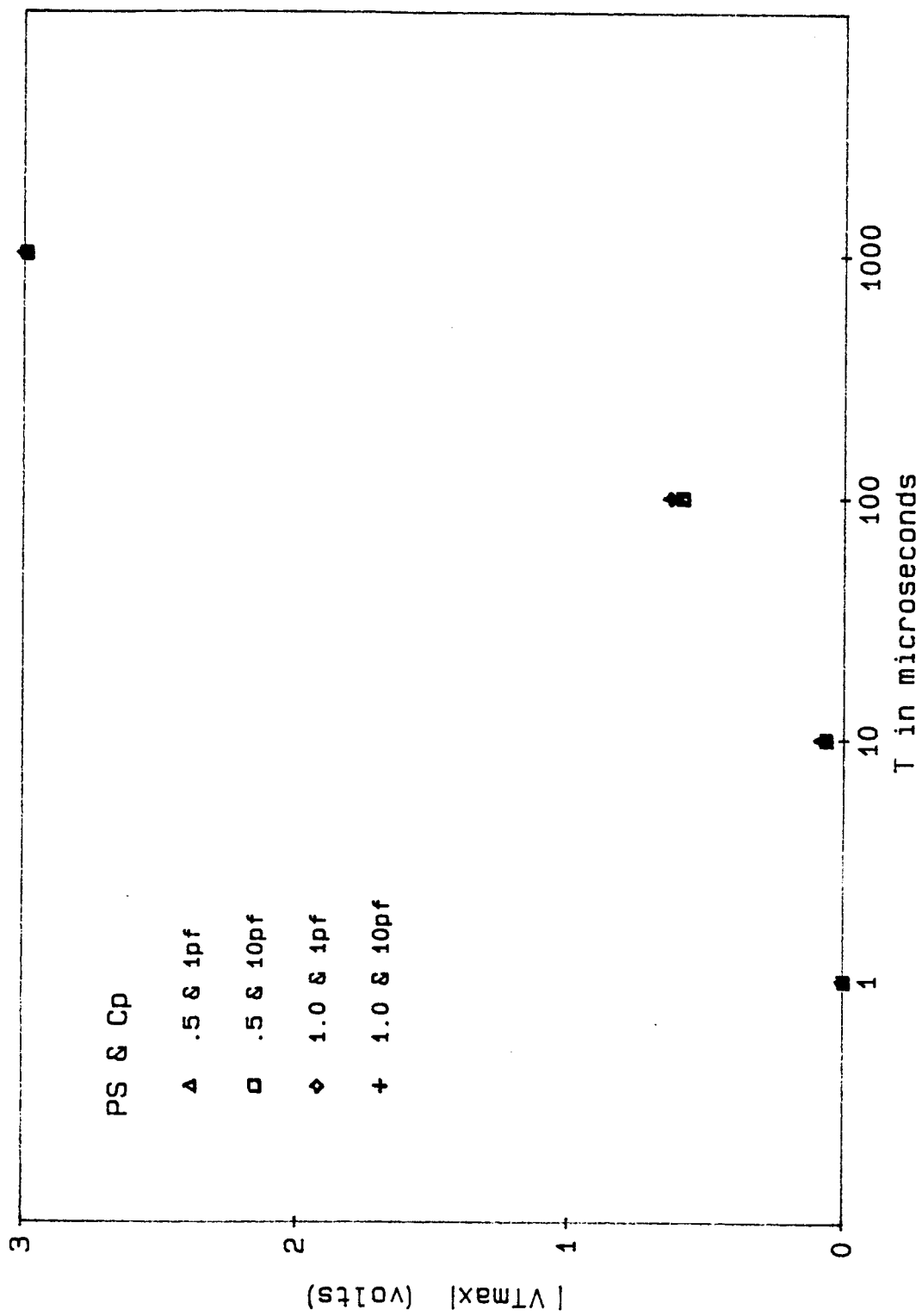


FIG. 13 -  $V_{Tmax}$  vs  $f$  (PF=.8,  $C_p=1\text{pf}$ )

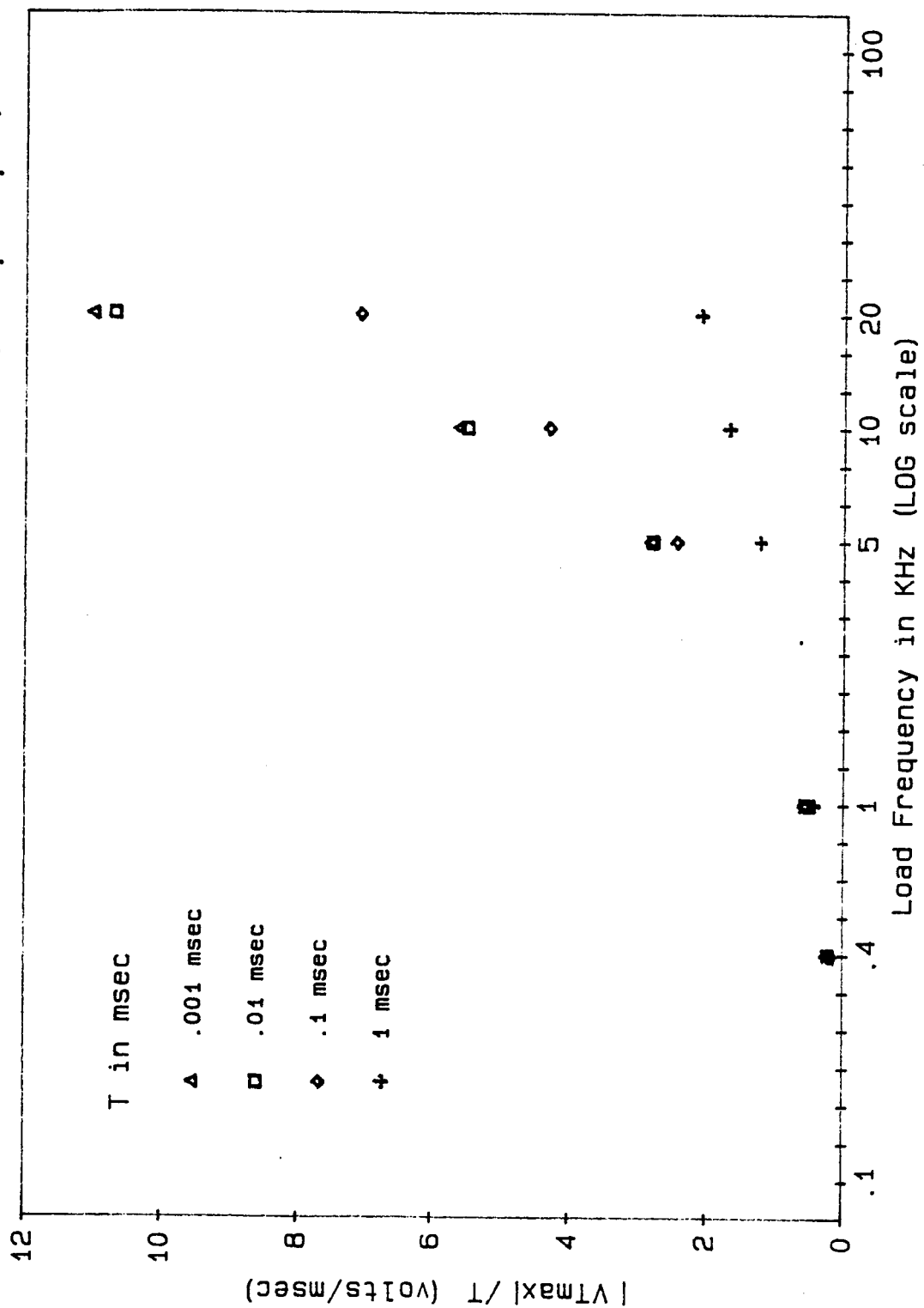


FIG. 14 -  $V_{Tmax}$  vs  $f$  (PF=1,  $C_p=1\text{pf}$ )

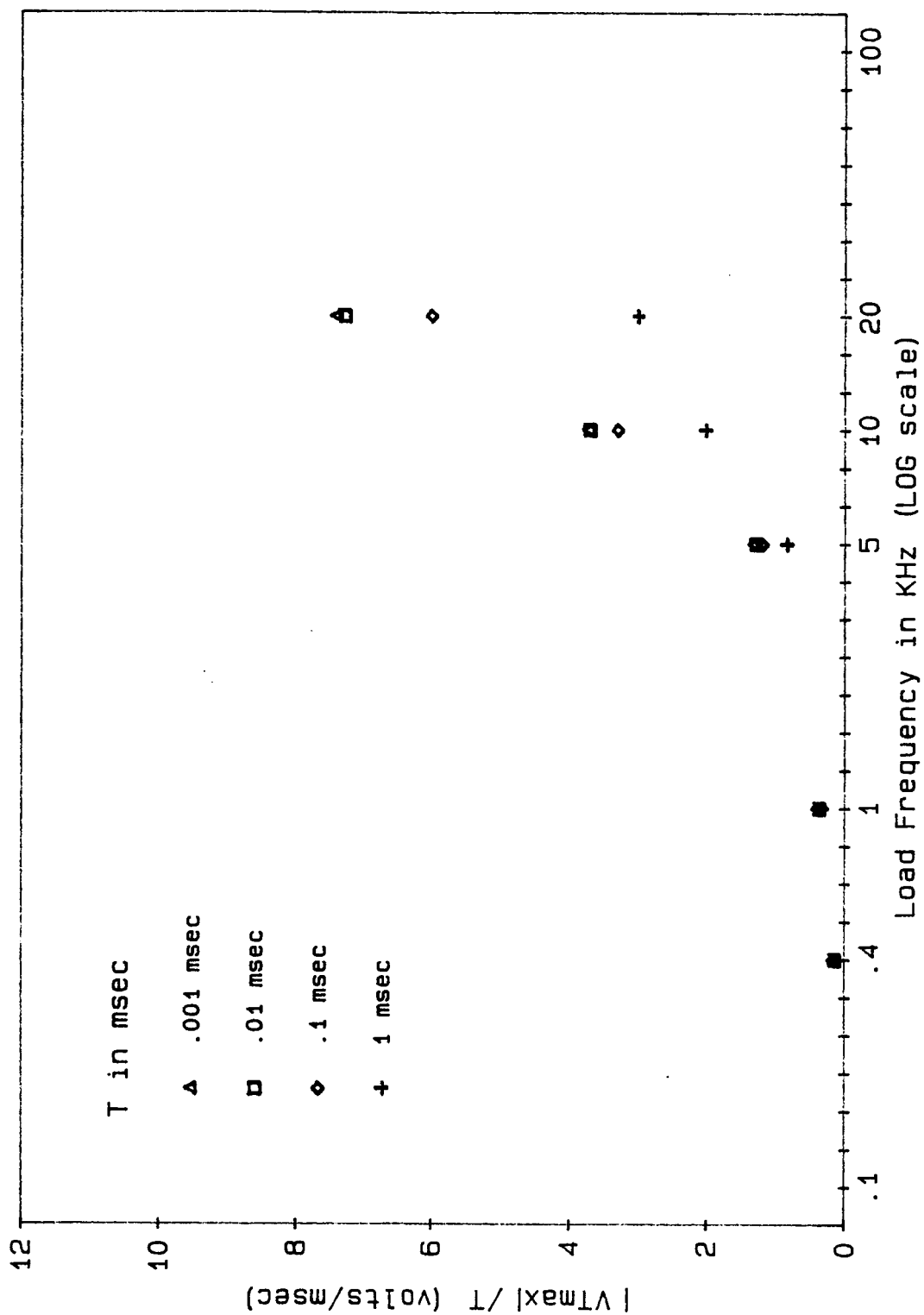


TABLE 1.

t=0 Solutions for 80% of Maximum Power and Thermal Ions

Pe	Pi	FF	Pmade	Ploss	VTmax	BBCmax
.5	.5	2.6%	65664W	42W	-7.3	0
1	.5	0.7%	65665W	43W	-7.3	0
1.2	.5	0.43%	65665W	43.5W	-7.3	0
.5	1	29%	66578W	1278W	-7.4	0
1	1	7.9%	67248W	2196W	-8	0
1.2	1	5%	67350W	2336W	-8	0
.5	1.2	50%	67685W	2800W	-7.8	0
1	1.2	16.3%	71721W	8647W	-9	0
1.2	1.2	10.3%	72590W	9997W	-10	0

Io = 50 amps

T = 10 microseconds

Cp = 10 pf

K = 5

TABLE 2.

t=0 Solutions for 80% of Maximum Power and Ram Ions (5ev)

Pe	Pi	FF	Pmade	Ploss	VTmax	BBCmax
.5	.5	4.1%	65687W	74W	-7	0
1	.5	1.2%	65690W	77W	-7.6	0
1.2	.5	0.7%	65690W	78W	-7.5	0
.5	1	14.6%	65988W	478W	-7.4	0
1	1	3.9%	66087W	613W	-7.4	0
1.2	1	2.5%	66101W	630W	-8	0
.5	1.2	22%	66290W	887W	-7.3	0
1	1.2	6%	66642W	1365W	-7.6	0
1.2	1.2	3.9%	66694W	1436W	-8	0

Io = 50 amps

T = 10 microseconds

Cp = 10 pf

K = 5

TABLE 3.

t=0 Solutions for 100% of Maximum Power and Thermal Ions

Pe	Pi	FF	Pmade	Ploss	VTmax	BBCmax
.5	.5	2.65%	82045W	35W	-22	20
1	.5	0.8%	82045W	36W	-22	20
1.2	.5	0.46%	82045W	36W	-22	20
.5	1	28%	82013W	1016W	-21	20
1	1	7.9%	81947W	1692W	-20	-10
1.2	1	5.1%	81933W	1796W	-20	10
.5	1.2	48.3%	81858W	2205W	-20	10
1	1.2	16.1%	80255W	6027W	-18	0
1.2	1.2	10.3%	79628W	6789W	-19	0

Io = 50 amps

T = 10 microseconds

Cp = 10 pf

K = 5

TABLE 4.

t=0 Solutions for 100% of Maximum Power and Ram Ions (5ev)

Pe	Pi	FF	Pmade	Ploss	VTmax	BBCmax
.5	.5	4%	82045W	62W	-22	20
1	.5	1.2%	82045W	64W	-23	20
1.2	.5	0.8%	82045W	65W	-22	20
.5	1	14%	82042W	380W	-22	20
1	1	3.9%	82040W	480W	-21	20
1.2	1	2.6%	82040W	493W	-22	20
.5	1.2	21%	82032W	694W	-21	20
1	1.2	6%	82014W	1039W	-21	10
1.2	1.2	3.9%	82010W	1090W	-21	20

$I_o = 50$  amps  
 $T = 10$  microseconds  
 $C_p = 10$  pf  
 $K = 5$